Conductive "Smart" Hybrid Hydrogels with PNIPAM and Nanostructured Conductive Polymers

*Ye Shi, Chongbo Ma, Lele Peng, and Guihua Yu**

Stimuli-responsive hydrogels with decent electrical properties are a promising class of polymeric materials for a range of technological applications, such as electrical, electrochemical, and biomedical devices. In this paper, thermally responsive and conductive hybrid hydrogels are synthesized by in situ formation of continuous network of conductive polymer hydrogels crosslinked by phytic acid in poly(*N*-isopropylacrylamide) matrix. The interpenetrating binary network structure provides the hybrid hydrogels with continuous transporting path for electrons, highly porous microstructure, strong interactions between two hydrogel networks, thus endowing the hybrid hydrogels with a unique combination of high electrical conductivity (up to 0.8 S m^{-1}), high thermoresponsive sensitivity (significant volume change within several seconds), and greatly enhanced mechanical properties. This work demonstrates that the architecture of the filling phase in the hydrogel matrix and design of hybrid hydrogel structure play an important role in determining the performance of the resulting hybrid material. The attractive performance of these hybrid hydrogels is further demonstrated by the developed switcher device which suggests potential applications in stimuli-responsive electronic devices.

1. Introduction

"Smart" hydrogels which are sensitive to external stimuli such as temperature,[1] pH,[2] electric field,[3,4] magnetic force,[5] *etc.* could react actively to environment changes,[6] thus receiving increasing attention in recent years. However, traditional smart hydrogels are generally electrically nonconductive[7] while conductive gels hold great promise for a wide range of applications in sensors,[8,9] fuel cells,[10] supercapacitors,[11–16] dye-sensitized solar cells,[17–19] and lithium batteries.[20,21] The conductive responsive hydrogels could be fabricated by incorporation of a second ingredient such as conducting fillers,[22] conductive polymers,[23] or carbon based gel-like materials[7,24] into the gel matrix, forming hybrid "smart" hydrogels with stimuli-responsive properties and conductivity.

Adding conducting nanofillers such as carbon nanotubes,[25,26] carbon black,[27] and metal nanoparticles[28] to polymer hydrogels has been widely adopted to enhance the conductivity of hydrogels. As nanofillers tend to aggregate and are randomly distributed in polymer matrix, surface functionalization and large amount of the fillers are needed to help them form a continuous, electrically conductive network.[29] This blending method usually weakens the mechanical properties of the conductive hybrid gels and reduces the stimuli-responsiveness due to the restricted motion of polymer chains by strong interaction between fillers and the polymer matrix.[30] Conductive polymers such as polyaniline (PANI) and polypyrrole (PPy) have also been incorporated into gel systems. However, traditionally synthesized hybrid gel consisting of conductive polymers and stimuli-responsive hydrogels usually possesses the structure of separate domains of conductive polymers dispersed within porous polymer matrix, lowering the electrical performance of the hybrid gel.[23] Recently, conductive smart hydrogels have been synthesized by introducing graphene aerogels.[7] The resulting hybrid hydrogel holds robust mechanical performance and decent electrical properties. Alternatively, the adoption of conductive polymers is another facile and low-cost method to synthesize smart hydrogels with good conductivity and mechanical properties because it is less complicated and costly compared to the synthesis of graphene aerogels.

In this paper, we introduced the conductive polymer hydrogels into a widely studied thermally responsive hydrogel, poly(*N*-isopropylacrylamide) (PNIPAM), and developed the conductive smart gels sensitive to temperature change. Despite the traditional hybrid gel of randomly dispersed conductive polymer and stimuli responsive hydrogels, a mesh-like hydrogel network of conductive polymer could be in situ formed due to the phytic acid molecule which can react with more than one PANI (or PPy) chain by protonating the nitrogen groups on PANI (or PPy) and thus promote the crosslinked structure.[13] The formation of conductive network can avoid surface modification which inhibits the aggregation of polymer particles and can provide continuous conducting paths for electron transport, thus enhancing the conductivity of hybrid hydrogel. The mechanical properties could be also improved due to the interaction between two hydrogel networks. The porous nature of the hybrid hydrogel we obtained can maintain the thermal sensitivity of PNIPAM hydrogel because the water can easily flow

Y. Shi, C. Ma, L. Peng, Prof. G. Yu
Materials Science and Engineering Program
and Department of Mechanical Engineering
Texas Materials Institute
The University of Texas at Austin
TX 78712, USA
E-mail: ghyu@austin.utexas.edu

DOI: 10.1002/adfm.201404247

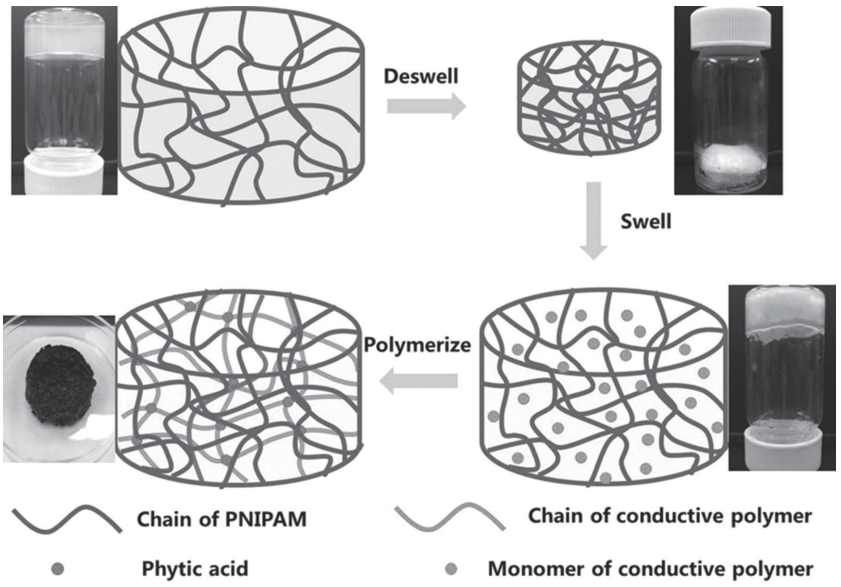

Figure 1. Schematic illustration of synthesis process of hybrid hydrogel composed of PNIPAM and conductive polymers. The deswelled PNIPAM hydrogel is immersed into the solution of monomers of conductive polymer and absorbs the monomers until it reswells to original volume. Then the reswelled hydrogel is immersed into the solution of oxidative initiator and phytic acid, allowing the in situ polymerization and crosslinking of conductive polymer chains. The photos show different states of hydrogels.

within pores. The combination of conductive polymer hydrogel and thermally responsive hydrogel renders the hybrid gel high electronic property and responsive sensitivity which are demonstrated by a fabricated switcher that can sensitively respond to the change of temperature.

2. Results and Discussion

The synthesis process and gelation mechanism of hybrid hydrogel is illustrated in **Figure 1**. The unique coil-to-globule transition of PNIPAM chains at the lower critical solution temperature (LCST) (around 35 °C)[32] allows the large temperature-responsive volume phase transition of the hydrogel and loss of large amount of water. The deswelled hydrogel is immersed into solution of monomers of conductive polymer, thus absorbing the monomers until it reswells to original volume. Then the reswelled hydrogel containing monomers of conductive polymer is immersed into the solution of oxidative initiator and phytic acid, allowing in situ polymerization and crosslinking of conductive polymer chains. Phytic acid, an abundant natural product found in plants,[33] reacts with PANI or PPy chains by protonating the nitrogen groups; one phytic acid molecule can interact with more than one conductive chain, thus resulting in the formation of hydrogel network. The amount of conductive hydrogel in hybrid gel could be easily tuned by controlling the concentration of monomer solution used in the reswelling process. The formation of hybrid hydrogels could be verified by the UV–vis spectra of PNIPAM, PNIPAM/PANI and PNIPAM/PPy hydrogels (Figure S1, Supporting Information). The hybrid gels of PNIPAM/PANI and PNIPAM/PPy exhibit high absorbance in the range of visible light, which is consistent with their colors (dark green for PNIPAM/PANI and black for PNIPAM/PPy).

The morphology and microstructure of hybrid hydrogels of PNIPAM/PANI and PNIPAM/PPy were investigated by scanning electron microscope (SEM). **Figure 2**a shows the SEM image of freeze dried PNIPAM/PANI. We can find the porous structure of the hybrid hydrogel and the size of pores ranges from several micrometers to larger than 10 micrometers. Such hierarchical porous structures provide both large open channels between the branches and nanoscale porosities within the structures which facilitate the transport of water molecules. The hybrid gel of PNIPAM/PPy shows a different morphology which is illustrated in Figure 2b. The structure of interconnected spheres with size around 200 nm is a typical microstructure of the PPy hydrogel. Among the spheres, materials with smooth surface can be found and they can be identified as PNIPAM. The formation of spherical geometry

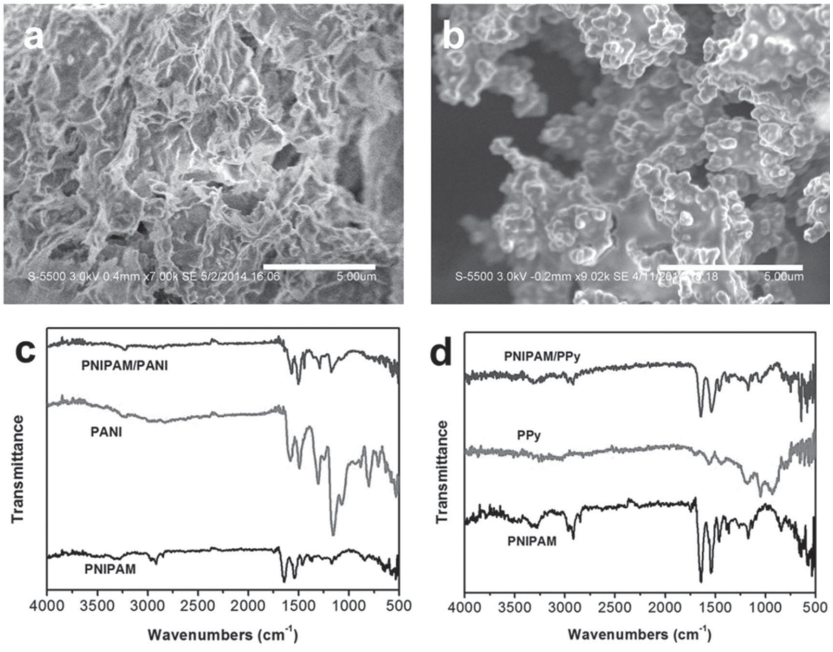

Figure 2. SEM images of a) PNIPAM/PANI and b) PNIPAM/PPy hybrid hydrogels. c) FTIR spectra of PNIPAM, PANI, and PNIPAM/PANI hydrogels. d) FTIR spectra of PNIPAM, PPy, and PNIPAM/PPy hydrogels.

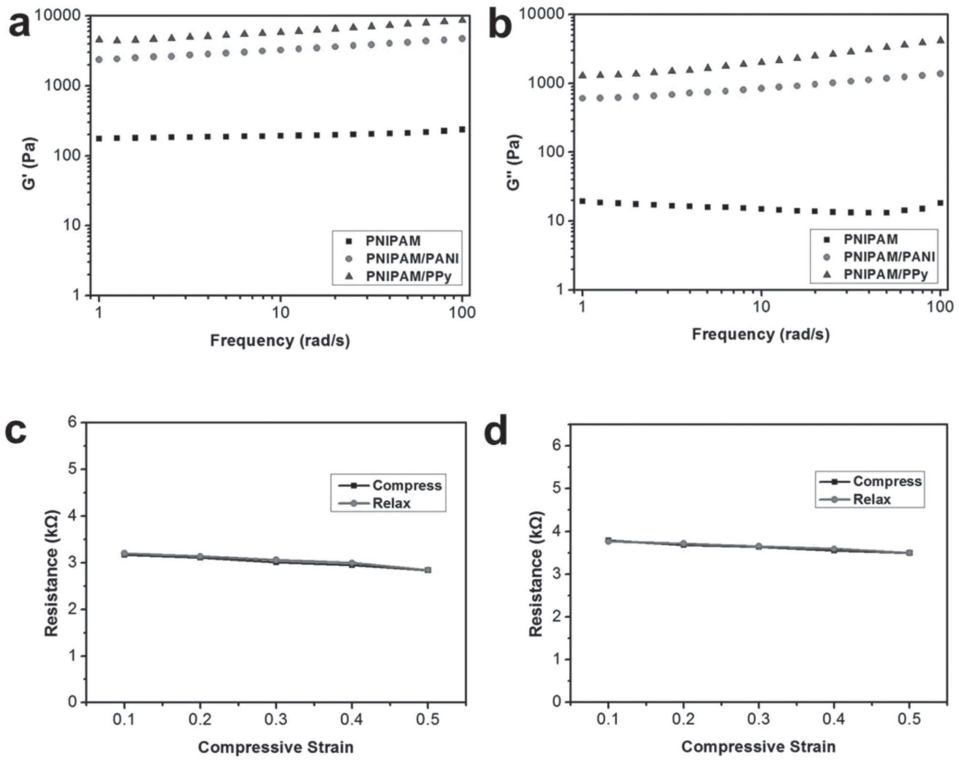

Figure 3. a,b) The storage modulus (G′) and loss modulus (G″) of PNIPAM, PNIAPM/PANI, and PNIPAM/PPy hydrogels tested in a frequency sweep mode. c,d) Resistance of PNIPAM/PANI and PNIPAM/PPy cylinder-shaped hybrid hydrogels at different strains, respectively. The consistent values in compressing and relaxing cycles demonstrate excellent electrical stability of hybrid hydrogels under deformation.

with a structural hierarchy could overcome the rigid nature of PPy chains and endows the hydrogel with effective elasticity.[12] Overall, the hybrid gel of PNIPAM/PPy also possesses a highly porous structure with pores ranging from several micrometers to larger than 10 μm, thus facilitating the flowing of water and ensuring the high sensitivity of hybrid gels.

The chemical structures of as-synthesized hybrid hydrogels of PNIPAM/PANI and PNIPAM/PPy were analyzed by the Fourier transform infrared (FTIR) spectra. Figure 2c shows the FTIR spectra of PNIPAM, PANI, and PNIPAM/PANI. In the spectrum (black) of PNIAPM, peaks at 1540 and 1645 cm^{-1} can be attributed to N–H bending and C=O stretching, which are both characteristic of PNIPAM.[34] The spectrum (red) of PANI indicates that it is the emeraldine salt form of PANI with two characteristic absorption peaks at 1570 and 1480 cm^{-1} corresponding to the stretching vibration of the quinoid ring and benzenoid ring, respectively.[13] All the characteristic peaks of PNIPAM and PANI can be found in the FTIR spectrum of synthesized hybrid hydrogel of PNIPAM and PANI, confirming the formation of composites of PNIPAM and PANI. For the identification of hybrid gel of PNIPAM and PPy, the typical FTIR spectra of PNIPAM, PPy and PNIPAM/PPy are shown in Figure 2d. The spectrum of PPy shows the absorption peak at 1552 cm^{-1} corresponding to the in-ring stretching of C=C bonds in the pyrrole rings and the peak at 1045 cm^{-1} which can be attributed to the in-plane deformation of N–H bond.[12] These two characteristic peaks can also be found in the FTIR spectrum of as-synthesized hybrid hydrogel, confirming the formation of PPy in the PNIPAM matrix and the successful synthesis of PNIPAM/PPy. We also found that the chemical structures of PANI and PPy within hybrid hydrogels are well maintained confirmed by the PNIPAM subtracted FTIR spectra of conductive hybrid hydrogels (Figure S2, Supporting Information).

Desirable mechanical properties are important for responsive hydrogels, especially when they are applied in practical devices.[35] Hydrogels are viscoelastic materials and they exhibit the properties of storing and dissipation of energy.[6] The amount of energy stored in the gel system and the amount of energy dissipated within the system under the oscillatory stress are indicated by the storage modulus (G′) and the loss modulus (G″), respectively. The G′ and G″ values of PNIPAM, PNIPAM/PANI and PNIPAM/PPy are shown in **Figure 3**a,b. The dynamic frequency sweep experiments of all three gels show a wide linear viscoelastic region. And the value of storage modulus is higher than that of the loss modulus in each case, confirming their gel state. The G′ values of both hybrid hydrogels are significantly higher than that of pure PNIPAM hydrogel and PNIPAM hydrogel after swelled in monomers of aniline and pyrrole but before polymerization (Figure S3, Supporting Information), indicating the increased strength. This is resulted from the reinforcement effect induced by the formation of a continuous and mechanically efficient network of conductive polymer with rigid backbones. The covalent bond of PANI and PPy chains facilitates dissipation of energy. The interactions between two networks of hydrogels also contribute to the increase of mechanical strength of hybrid hydrogels.

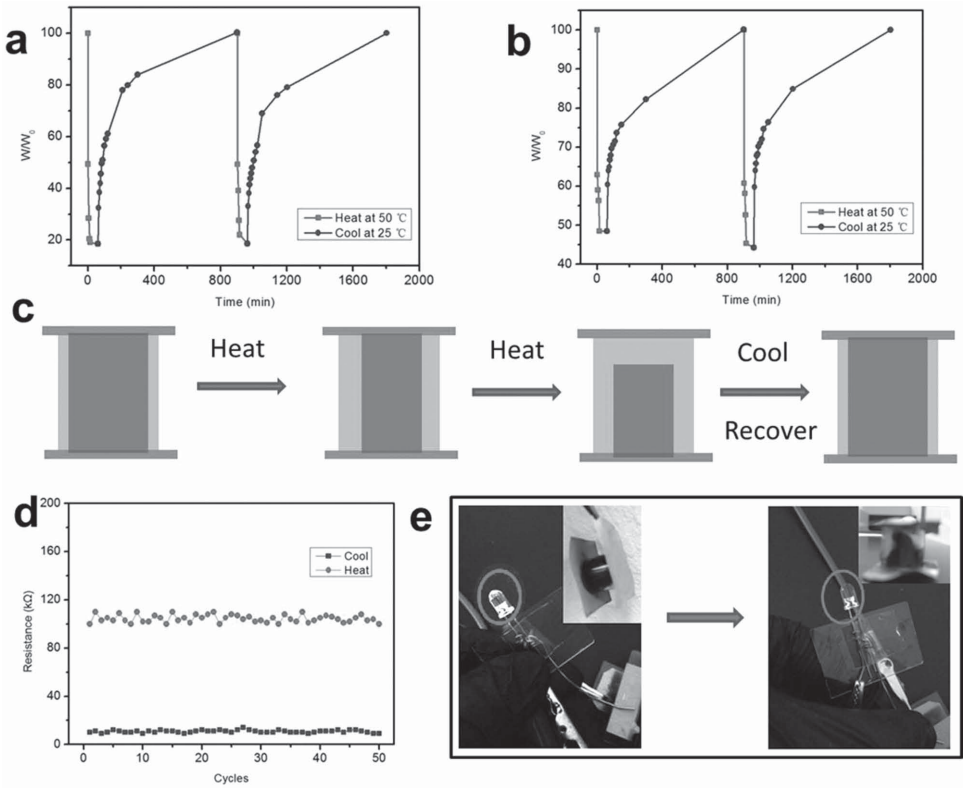

Figure 4. The swelling and deswelling behavior of PNIPAM/PANI a) and PNIPAM/PPy b) hybrid hydrogels. c) Schematic of working mechanism of the switcher device based on thermal-responsive conductive hydrogels. d) Cycling performance of the switcher device. e) The demo circuit in which the on/off states of LED is controlled by the close-circuit/open-circuit states of the electrical circuit which is determined by the states of switcher. The inset photographs show the swelled and deswelled states of hybrid hydrogels in the device.

The elasticity (G′–G″)[36] calculated from the rheological data are 157, 1763, and 3231 Pa for PNIPAM, PNIPAM/PANI, and PNIPAM/PPy hydrogels, respectively. The hybrid hydrogels possess increased elasticity due to the foam-like structure of PANI hydrogel and spherical geometry of PPy hydrogel which are consistent with the morphologies shown in SEM pictures. Ten cycles of compression and tension tests for PNIPAM, PNIPAM/PANI, and PNIPAM/PPy hydrogels were conducted and the results are shown in Figure S4, Supporting Information. The modulus can be calculated as 36.7, 66.1, and 54.5 Pa for PNIPAM, PNIPAM/PANI, and PNIPAM/PPy hydrogels, respectively. The modulus of hybrid gels are both enhanced when compared to that of pure PNIPAM and all these modulus values are typical for hydrogels with high water content. The narrow gap between compression and tension curve for hybrid gels indicate that they can recover quickly. The cycling performance of PNIPAM, PNIPAM/PANI, and PNIPAM/PPy hydrogels (Figure S4b–d, Supporting Information) demonstrated that excellent elasticity is well maintained for hybrid gels. The enhanced mechanical properties of hybrid hydrogels are further revealed by the fracture experiments. When fractured, the pure PNIPAM hydrogel breaks into small pieces while the hybrid hydrogels show a single large crack, indicating that the binary network structure of hybrid hydrogel combining PNIPAM and conductive polymer hydrogels contributes to the relax of local stress and dissipation of microcrack energy.

We further designed a test to demonstrate the stability of electrical properties of the hybrid hydrogels under mechanical strain. The cylinders of PNIPAM/PANI and PNIPAM/PPy hydrogels with thickness of 5 mm are compressed by 0.5 mm each time and the largest strain reaches 50%. Figure 3c,d shows the changes of resistance for PNIPAM/PANI and PNIPAM/PPy hydrogels during the compressing test, respectively. We can find that the resistance of both hybrid hydrogels remains almost constant during compressing and relaxing cycle. Even under strain as large as 50%, the decrease of resistance is rather small (<1%), indicating the excellent electrical stability of hybrid hydrogels under mechanical deformation.

For practical applications, the thermally responsive functions of PNIPAM hydrogel should not be negatively affected by the incorporation of conductive polymers. **Figure 4**a,b shows the swelling and deswelling behavior of PNIPAM/PANI and PNIPAM/PPy hybrid hydrogels. PNIPAM/PANI shows a large swelling ratio of 5.2, while PNIPAM/PPy shows a lower swelling ratio of 2.3 which is still reasonable for thermoresponsive application. The difference of swelling ratios between PNIPAM/PANI and PNIPAM/PPy is induced by the different morphologies of two hybrid hydrogels. The PPy hydrogel forms particles with smaller size when compared to the mesh-like structure of PANI hydrogel, thus filling more space in the PNIPAM matrix and resulting in a lower swelling ratio. Besides the swelling ratio, responsive sensitivity is another important factor for thermally responsive hydrogels. As shown in Figure 4a,b, sharp

decrease of mass happens for both two hybrid hydrogels when immersed in water with temperature of 50 °C, demonstrating high sensitivity to thermal stimuli. The conductive hybrid hydrogels almost reach the largest degree of deswelling within 1 min. In the recovering half cycle, both the hybrid hydrogels exhibit a sharp increase of mass during the first several minutes. Then swelling slows down until it takes about 15 h to recover to original swelled status. The swelling and deswelling behavior of hybrid hydrogels is consistent with that of PNIPAM hydrogel, confirming the unaffected responsive function of hydrogels after incorporation of conductive polymers. The good thermoresponsive behavior of hybrid hydrogels can be mainly ascribed to their interpenetrating binary network structure and porous nature which reduce the restriction of PNIPAM chains and facilitates the flow of water molecules within the hydrogel network. The region exhibiting vertical change of mass in the swelling and deswelling curves suggests the excellent thermoresponsive sensitivity of the designed hybrid hydrogels and ensures their application in responsive devices.

Apart from the enhanced mechanical properties and well-preserved thermoresponsive sensitivity, the hybrid hydrogels based on PNIPAM and conductive polymers exhibit excellent electrical properties. By using the four-probe method, we measured the bulk electrical conductivities of PNIPAM/PPy and PNIPAM/PANI hydrogels each for ten samples and their conductivities are 0.15 ± 0.03 and 0.84 ± 0.02 S m^{-1} at the gel state (Figure S5, Supporting Information), respectively. We also noticed that conductivity decreases as the temperature increases for both hybrid hydrogels. This may be caused by the change of swelling states and microstructures (Figure S6, Supporting Information). The higher conductivity of PNIPAM/PPY hydrogel may be due to the higher loading of PPy in the hybrid gel which is revealed by the lower swelling ratio of PNIPAM/PPy gel. Pure conducting polymer hydrogels typically show the electrical conductivity in the range of 0.01–1 S m^{-1} and the highest value reported is 11 S m^{-1} for the PANI hydrogel synthesized by phytic acid as the crosslinker.[37] However, recent literature reported that the electrical conductivity significantly decreases when the conductive polymers are introduced into other responsive hydrogel systems. The PANI/folic acid[6] and tetraaniline/polyvinyl alcohol (PVA),[38] hemicellulose hydrogel/aniline pentamer[39] hybrid hydrogel exhibit a conductivity of 0.0014, 0.001, and 9.05×10^{-7}–1.58×10^{-4} S m^{-1}, respectively and the PANI particles/PNIPAM hybrid hydrogel[23] shows a conductivity in the range of 0.0045–0.027 S m^{-1}. Compared to these smart hydrogel systems with conductive polymers incorporated, the electrical conductivities of our hybrid hydrogels are approximately two orders of magnitude higher and close to those of pure conductive polymers, demonstrating excellent electrical properties. What is more, our conductive hybrid hydrogels also show comparable electrical performance to PNIPAM based conductive hydrogel[7] recently developed by Li *et al.* which exhibited remarkable electrical conductivity in the range of 0.7–10 S m^{-1} by adding different amounts of graphene aerogel (the electrical properties of different hydrogels are summarized in **Table 1**). The excellent electrical properties of our hybrid hydrogels could be attributed to the in situ formation of networks of conductive polymers which can act as the continuous transporting path for electrons. In contrast, hybrid hydrogels based on randomly dispersed conductive particles or monomers consist of point-to-point connected conducting network resulting in a poor electrical conductivity. The enhanced mechanical performance, high thermoresponsive and electrical properties of our hybrid hydrogels open up new opportunities for exploring the applications of conductive smart hydrogels.

Table 1. Electrical conductivities of conductive hydrogels.

Conductive hydrogels	Electrical conductivity [S m^{-1}]
Our PPy/PNIPAM	0.8
Our PANI/PNIPAM	0.2
PANI hydrogel crosslinked by phytic acid[31]	11
PNIPAM/graphene[6]	0.7–10
Typical conductive polymer[31]	0.01–1
PANI/folic acid[5]	0.0014
PANI domains/PNIPAM[19]	0.0045–0.027
Tetraaniline/PVA[32]	0.001
Hemicellulose hydrogel/aniline pentamer[39]	9.05×10^{-7}–1.58×10^{-4}

Based on the thermoresponsive and conductive properties of hybrid hydrogels, we designed a thermally responsive switcher. As shown in Figure 4c, a certain amount of hybrid hydrogel is sealed into a cylinder shell with top and bottom electrodes. The hydrogel and electrodes are well contacted at first and thus it becomes a conductor. When the switcher is heated, the hybrid hydrogel shrinks due to the deswelling. The resistance of the switcher device increases due to the conductivity change of hybrid hydrogel which is caused by the loss of water within hydrogel matrix and the decrease of contacting area between conductive hydrogels and the electrodes. When the device is further heated, the hydrogel continuously shrinks and finally loses contact with electrodes, thus switching to open-circuit status. The device could revert to close-circuit status when the temperature is cooled down. The hybrid hydrogels swell under LCST and recreate the electrical contact between conductive hydrogels and electrodes, thus forming a transporting path for current. The "switching" behavior could be completed within 10 s due to the excellent responsive sensitivity of hybrid hydrogels, ensuring the quick response of switcher device to temperature change.

The cycling performance of the switcher is further tested to demonstrate the stability of conductive hydrogel based switcher device. Figure 4d shows the 50 cycles of heating and cooling of the switcher. The resistance of switcher maintains around 110 kΩ at heated (deswelled) status and stays around 10 kΩ at cooled (swelled) status even after 50 cycles. The excellent cycling performance is supported by the good mechanical properties and electrical stability of the hybrid hydrogels. The change of resistance occurs within 10 s after the device is heated or cooled, demonstrating the highly thermoresponsive sensitivity of the hybrid hydrogels. The difference of resistance at deswelled and swelled states is significant, ensuring the "switching" behavior of the device under thermal stimuli.

And the resistance difference could be tuned by controlling the amount of hybrid hydrogels sealed in between the two electrodes. The switcher can function between totally open-circuit and close-circuit states by losing and recreating the contact between conductive hybrid hydrogel and electrodes. The demonstrated circuit is shown in Figure 4e in which the on/off states of light emitting diode (LED) is controlled by the close-circuit/open-circuit states of the electrical circuit which is determined by the states of switcher. The inset photographs show the swelled and deswelled states of hybrid hydrogels in the device. When the hydrogel is swelled, the contact between hydrogel and electrode is created, building the transport path for current. When the temperature is raised and the hydrogel is deswelled, it totally loses its contact to electrode, thus inducing the open-circuit state. Although the switcher based on our conductive hybrid hydrogels is a simple demonstration for their application in electronic devices, it reveals the high thermoresponsive sensitivity, enhanced mechanical properties and good electrical performance of our hybrid hydrogels and provides a new sight for the applications of the conductive hybrid hydrogels.

3. Conclusion

In summary, we successfully synthesized PNIPAM/conductive polymer based hybrid hydrogels by the in situ formation of continuous network of conductive polymer hydrogels crosslinked by phytic acid in PNIPAM matrix. With the interpenetrating binary network structure, our hybrid hydrogels exhibit a unique combination of high electrical conductivity, high thermoresponsive sensitivity and enhanced mechanical properties. These unique properties are further demonstrated by the switcher device based on our hybrid hydrogels. Our work demonstrates that the architecture of the filling phase in the hydrogel matrix plays an important role in determining the performance of the resulting hybrid material. These hybrid hydrogels may find potential applications in stimuli-responsive electronic devices, self-adaptive electronics, and flexible bioelectronics.

4. Experimental Section

Preparation of Hybrid Hydrogels: The synthesis of PNIPAM was previously described in the literature. In a typical synthesis process, *N*-isopropylacrylamide monomers (283 mg), *N*′,*N*′-methylenebisacrylamide acting as crosslinker (15 mg), and deionized (DI) water (5 mL) were mixed together and purged with nitrogen gas for 5 min. Then ammonium persulfate (APS) (10 mg) and *N*′,*N*′-tetramethylenediamine acting as accelerator (5 mL) were added into the mixture and the polymerization was carried out for 12 h. The obtained PNIPAM hydrogel was immersed into DI water overnight to remove unreacted monomers. After cleaning, the PNIPAM hydrogel was heated at 50 °C to completely deswell and then immersed in aniline or pyrrole to be swelled again. The reswelled hydrogel was added into APS (283 mg) and phytic acid solution (0.921 mL) and the conductive polymer was formed by in situ polymerization within the porous structure of PNIPAM hydrogel. Finally, the obtained hybrid hydrogel was immersed in DI water to remove unreacted residues.

Characterizations of Hybrid Hydrogels: The morphology and microstructure of samples were observed by Scanning Electron Microscopy (Hitachi, S5500) operating at 5 kV. Before observation, the hydrogels were freeze dried for 24 h. The FTIR spectra of hydrogels were recorded by the FTIR Spectrometer (Thermo Mattson, Infinity Gold FTIR) equipped with a liquid nitrogen cooled narrow band mercury cadmium telluride (MCT) detector, using attenuated total reflection cell equipped with a Ge crystal. To understand the mechanical properties of hydrogels, rheological experiments were performed by a rheometer (AR 2000EX, TA instrument) using parallel plate on a peltier plate in a frequency sweep mode. The temperature is 25 °C. The swelling and deswelling experiments were performed by immersing hydrogels in water at 25 and 50 °C. At specific times the hydrogel samples were picked and weighted after the water on the surface was removed. The electrical conductivity of hybrid hydrogels was tested by the four-probe method using a sourcemeter (Model 2400, Keithley) and then calculated by using the equations for bulk material below. The distance between each two probes was set as 1 mm. S_1 refers to the distance between probe 1 and probe 2. S_2 refers to the distance between probe 2 and probe 3. S_3 refers to the distance between probe 3 and probe 4.

$$\rho = \frac{V}{I}C$$

$$C = \frac{20}{\frac{1}{S_1}+\frac{1}{S_2}-\frac{1}{S_1+S_2}-\frac{1}{S_3+S_2}}$$

For the test of stability of electrical properties of the hybrid hydrogels under mechanical strain, we used the rheometer to compress the hydrogel sample. The cylinders of PNIPAM/PANI and PNIPAM/PPy hydrogels with thickness of 5 mm were place on the plate of rheometer and then compressed by 0.5 mm each time and the largest strain reaches 50%. The resistance was obtained by using a multimeter.

Supporting Information

Supporting Information is available from the Wiley Online Library or from the author.

Acknowledgements

Y.S. and C.M. contributed equally to this work. The authors thank Prof. Joseph H. Koo and Prof. Christopher J. Ellison at the University of Texas at Austin for instrumental support and valuable discussions. The authors acknowledge the support from the startup grant from the University of Texas at Austin, Ralph E. Junior Faculty Award grant, and The Welch Foundation grant F-1861.

Received: December 1, 2014
Published online: January 14, 2015

[1] D. Li, X. Zhang, J. Yao, G. P. Simon, H. Wang, *Chem. Commun.* **2011**, *47*, 1710.
[2] L. P. Lv, K. Landfester, D. Crespy, *Chem. Mater.* **2014**, *26*, 3351.
[3] N. Annabi, A. Tamayol, J. A. Uquillas, M. Akbari, L. E. Bertassoni, C. Cha, G. Camci Unal, M. R. Dokmeci, N. A. Peppas, A. Khademhosseini, *Adv. Mater.* **2014**, *26*, 85.
[4] X. Yang, L. Qiu, C. Cheng, Y. Wu, Z. F. Ma, D. Li, *Angew. Chem. Int. Ed.* **2011**, *50*, 7325.
[5] Y. D. Liu, H. J. Choi, *Polym. Int.* **2013**, *62*, 147.
[6] P. Chakraborty, P. Bairi, B. Roy, A. K. Nandi, *ACS Appl. Mater. Interfaces* **2014**, *6*, 3615.
[7] L. Qiu, D. Liu, Y. Wang, C. Cheng, K. Zhou, J. Ding, V. T. Truong, D. Li, *Adv. Mater.* **2014**, *26*, 3333.
[8] L. Pan, A. Chortos, G. Yu, Y. Wang, S. Isaacson, R. Allen, Y. Shi, R. Dauskardt, Z. Bao, *Nat. Commun.* **2014**, *5*, 3002.

[9] D. Zhai, B. Liu, Y. Shi, L. Pan, Y. Wang, W. Li, R. Zhang, G. Yu, *ACS Nano* **2013**, *7*, 3540.
[10] J. Ma, N. A. Choudhury, Y. Sahai, R. G. Buchheit, *J. Power Sources* **2011**, *196*, 8257.
[11] L. Zhang, G. Shi, *J. Phys. Chem. C* **2011**, *115*, 17206.
[12] Y. Shi, L. Pan, B. Liu, Y. Wang, Y. Cui, Z. Bao, G. Yu, *J. Mater. Chem. A* **2014**, *2*, 6086.
[13] L. Pan, G. Yu, D. Zhai, H. R. Lee, W. Zhao, N. Liu, H. Wang, B. C. K. Tee, Y. Shi, Y. Cui, Z. Bao, *Proc. Natl. Acad. Sci. U.S.A.* **2012**, *109*, 9287.
[14] Y. Wang, X. Yang, L. Qiu, D. Li, *Energy Environ. Sci.* **2013**, *6*, 477.
[15] H. J. Ding, M. J. Zhong, Y. J. Kim, P. Pholpabu, A. Balasubramanian, C. M. Hui, H. K. He, H. Yang, K. Matyjaszewski, C. J. Bettinger, *ACS Nano* **2014**, *5*, 4348.
[16] D. O. Carlsson, G. Nystrom, Q. Zhou, L. A. Berglund, L. Nyholm, M. Stromme, *J. Mater. Chem.* **2012**, *22*, 19014.
[17] Y. Zhao, B. Liu, L. Pan, G. Yu, *Energy Environ. Sci.* **2013**, *7*, 1990.
[18] Q. Li, Q. Tang, L. Lin, X. Chen, H. Chen, L. Chu, H. Xu, M. Li, Y. Qin, B. He, *J. Power Sources* **2014**, *245*, 468.
[19] P. Li, S. Yuan, Q. Tang, B. He, *Electrochim. Acta* **2014**, *137*, 57.
[20] B. Liu, P. Soares, C. Checkles, Y. Zhao, G. Yu, *Nano Lett.* **2013**, *13*, 3414.
[21] H. Wu, G. Yu, L. Pan, N. Liu, M. T. McDowell, Z. Bao, Y. Cui, *Nat. Commun.* **2013**, *4*, 1943.
[22] C. H. Zhu, Y. Lu, J. Peng, J. F. Chen, S. H. Yu, *Adv. Funct. Mater.* **2012**, *22*, 4017.
[23] R. E. Rivero, M. A. Molina, C. R. Rivarola, C. A. Barbero, *Sens. Actuators, B* **2014**, *190*, 270.
[24] S. Ahadian, J. Ramon-Azcon, M. Estili, X. Liang, S. Ostrovidov, H. Shiku, M. Ramalingam, K. Nakajima, Y. Sakka, H. Bae, T. Matsue, A. Khademhosseini, *Sci. Rep.* **2014**, *4*, 4271.
[25] X. Zhang, C. L. Pint, M. H. Lee, B. E. Schubert, A. Jamshidi, K. Takei, H. Ko, A. Gillies, R. Bardhan, J. J. Urban, M. Wu, R. Fearing, A. Javey, *Nano Lett.* **2011**, *11*, 3239.
[26] Z. Chen, J. W. F. To, C. Wang, Z. D. Lu, N. Liu, A. Chortos, L. J. Pan, F. Wei, Y. Cui, Z. N. Bao, *Adv. Energy Mater.* **2014**, DOI: 10.1002/aenm.201400207.
[27] W. J. Chuang, W. Y. Chiu, H. J. Tai, *J. Mater. Chem.* **2012**, *22*, 20311.
[28] C. Wang, H. Wu, Z. Chen, M. T. McDowell, Y. Cui, Z. Bao, *Nat. Chem.* **2013**, *5*, 1042.
[29] H. Kim, A. A. Abdala, C. W. Macosko, *Macromolecules* **2010**, *43*, 6515.
[30] K. Haraguchi, H. J. Li, *Angew. Chem. Int. Ed.* **2005**, *44*, 6500.
[31] K. N. Plunkett, X. Zhu, J. S. Moore, D. E. Leckband, *Langmuir* **2006**, *22*, 4259.
[32] J. T. Zhang, S. X. Cheng, R. X. Zhuo, *Colloid Polym. Sci.* **2003**, *281*, 580.
[33] G. Fundueanu, M. Constantin, P. Ascenzi, *Acta Biomater.* **2010**, *6*, 3899.
[34] T. Munk, S. Baldursdottir, S. Hietala, T. Rades, M. Nuopponen, K. Kalliomäki, H. Tenhu, J. Rantanen, C. J. Strachan, *Polymer* **2013**, *54*, 6947.
[35] X. Zhao, *Soft Matter* **2014**, *10*, 672.
[36] P. Bairi, B. Roy, P. Routh, K. Sen, A. K. Nandi, *Soft Matter* **2012**, *8*, 7436.
[37] S. W. Cao, Y. J. Zhu, *J. Phys. Chem. C* **2008**, *112*, 6253.
[38] H. Huang, W. Li, H. Wang, X. Zeng, Q. Wang, Y. Yang, *ACS Appl. Mater. Interfaces* **2014**, *6*, 1595.
[39] W. Zhao, L. Glavas, K. Odelius, U. Edlund, A. C. Albertsson, *Chem. Mater.* **2014**, *26*, 4265.